

UDC 620.17:620.18:621.735:669.14.018.29

A STUDY OF THE MICROSTRUCTURE AND MECHANICAL PROPERTIES OF MEDIUM-CARBON STEEL 40KhGNM AFTER WARM SWAGING

O. K. Dedyulina,¹ G. A. Salishchev,¹ and A. S. Pertsev²

Translated from *Metallovedenie i Termicheskaya Obrabotka Metallov*, No. 3, pp. 7 – 12, March, 2016.

The effect of the temperature and degree of deformation during warm swaging on the evolution of the microstructure and mechanical properties of preliminarily quenched medium-carbon steel 40KhGNM is studied. It is shown that the deformation produces an ultrafine-grained structure with ferrite grains elongated over the longitudinal direction and fine distributed nanocarbitides.

Key words: swaging, medium-carbon steel, nanocarbitides, elongated ultrafine-grained structure, strength, ductility, impact toughness.

INTRODUCTION

Medium-carbon structural steels are used widely for the production of critical machine parts. The best combination of properties required for such parts (strength and ductility) is commonly provided by toughening, i.e., quenching followed by high tempering at 550 – 650°C. However, the requirements on the steels of this type become stricter with the development of machine building; they should resist impact loads in a wide range of operating temperatures. One of the directions improving the toughness of steels is the use of quenching from the two-phase range. It has been shown in [1] that complete hardening of medium-carbon steels followed by quenching from the intercritical temperature range and high tempering raises the impact toughness (by a factor of 3 – 5 at the test temperature of –60°C) and the ductility. However, this is accompanied by lowering of the strength in all the specimens studied.

The strength characteristics and the ductility grow simultaneously when the grains are refined [2 – 4]. A effective means for obtaining fine grains in metals is plastic deformation [5]. Application of quenching and tempering to steel Fe – 0.4% C – 2% Si – 1% Cr – 1% Mo in combination with rolling in the ferrite-cementite range has resulted in [6] in considerable growth in the impact toughness (by up to a factor of 16) and in the strength and ductility as compared to the parameters provided by traditional heat treatment. The im-

act toughness also increased substantially in the temperature range of the brittle-to-ductile transition. The authors of [6] associate these changes in the mechanical properties with formation of an extended ultrafine-grained structure containing fine carbides.

One more effective method to refine the structure is swaging (rotary forging), the action of which on the structure and mechanical properties of medium-carbon steels has not been studied. Swaging is a process of reduction by rotating hammers that successively strike the treated billet in a uniform and distributed manner. Since the strain is accumulated at low reductions, the structure is more uniform over the whole of the volume of the billet than under the continuous treatment techniques. Swaging requires less treatment time, provides a good condition of the surface and accurate size tolerance [7].

The aim of the present work was to study the effect of various swaging modes on formation of ultrafine-grained structure and mechanical properties in medium-carbon low-alloy steel 40KhGNM.

METHODS OF STUDY

We tested specimens of medium-carbon low-alloy steel 40KhGNM of the following chemical composition (in wt.%): 0.43 C, 0.63 Cr, 0.60 Mn, 0.72 Ni, 0.27 Mo, 0.41 Si, 0.0236 P, 0.0385 S. The bars having a ferrite-pearlite structure in the initial condition were subjected to quenching from 840°C for a martensitic structure. Then the billets were swaged in several stages. First they were deformed at 600°C

¹ Belgorod State National Research University, Belgorod, Russia (e-mail: gsal@mail.ru).

² Perm Research University of Technology, Perm, Russia.

to $\varepsilon \sim 1.2$ and cut into two parts, one of which was deformed at 600°C to a total true strain $\varepsilon \sim 2.2$ and $\varepsilon \sim 2.9$ and the other was deformed at 500°C to a total true strain $\varepsilon \sim 2.2$ and $\varepsilon \sim 2.9$. After each stage of the swaging the cooling was conducted in air to room temperature.

The specimens for studying the microstructure after the swaging were cut in longitudinal and transverse directions from the central part of the bars. Polished sections were prepared with progressive decrease in the grain size of the abrasive paper and finally polished against a diamond paste. The surface of the sections was etched in a reagent composed of 4% HNO_3 and 96% $\text{C}_2\text{H}_5\text{OH}$. The foils for studying the fine structure of the steel were fabricated using a Struers TenuePol device in an electrolyte consisting of 95% CH_3COOH and 5% HClO_4 at room temperature and a voltage of 45 V. The microstructure was studied under a FI Quanta-600 scanning electron microscope in the mode of diffraction of backscattered electrons for plotting EBSD maps. The low-angle boundaries (LAB) ($2 - 15^\circ$) were marked in all the EBSD maps by thin black lines; the high-angle boundaries (HAB) were marked by thick black lines. To analyze the fine structure we used a JEOL JEM 2100 transmission electron microscope with accelerating voltage 200 kV.

The tensile mechanical tests and the tests for impact toughness were performed at room and low temperatures. Cylindrical tensile specimens were cut from the central parts of the bars in the longitudinal direction according to the GOST 1497–84 Standard using an Instron 5882 testing machine. The impact specimens with a *V*-notch were also cut in the longitudinal direction according to GOST 9454–78, type No. 11, and tested in a pendulum impact machine.

RESULTS AND DISCUSSION

Figure 1 presents the microstructure of quenched steel 40KhGNM after heating to deformation temperature $T = 600^\circ\text{C}$. The microstructure is typical and consists of a fine dispersed ferrite-carbide mixture; the fraction of HAB is 73%; the primary carbides have an average size of 120 nm; the average size of the secondary carbides is 40 nm.

Swaging changes the microstructure of the steel substantially for an elongated ultrafine-grained (UFG) structure (see Fig. 2). The kinetics of the evolution of the microstructure over the cross section of a bar varies substantially upon changes in the treatment temperature, which seems to be a result of a nonuniform strain distribution. For this reason we studied the microstructure of specimens cut from the central region of the bars. Since the ferrite grains were strongly extended, we evaluated their size only in cross section.

Let us consider the special features of the evolution of the microstructure of the steel during swaging at 600°C . In the initial stage of the deformation with $\varepsilon \sim 1.2$ (Fig. 2*a* and *b*) the microstructure of steel 40KhGNM is mostly represented by ferrite grained elongated over the direction of the deformation; a substructure forms inside these grains. This is

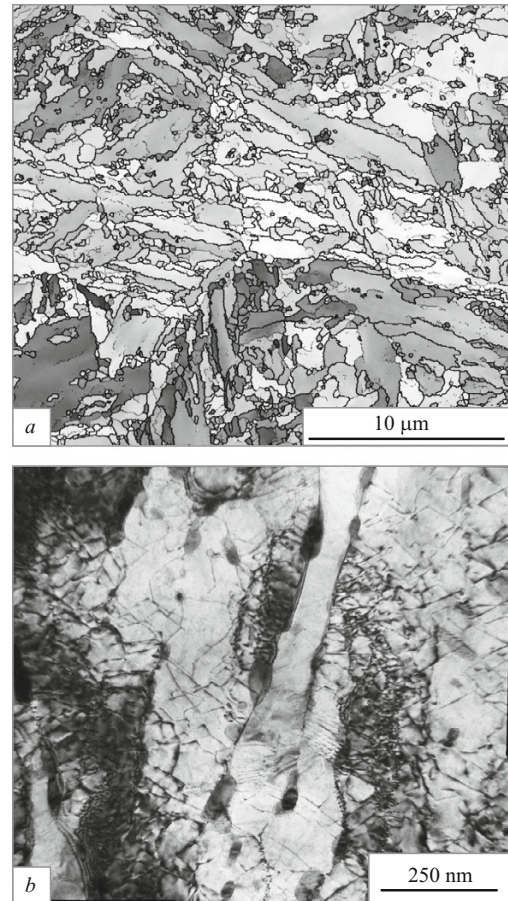


Fig. 1. Microstructure of steel 40KhGNM after quenching from 840°C and heating to the deformation temperature of 600°C : *a*) scanning electron microscopy in the EBSD mode; *b*) transmission electron microscopy.

accompanied by formation of new grains over ferrite boundaries. However, since the proportion of HAB decreases by 52% with respect to the initial value (Fig. 3*a*), this indicates weak development of recrystallization. The mean size of the grain-subgrain structure in cross section by the data of the EBSD is 420 nm; the mean size of the grains is 710 nm. When the strain increases to 2.2 (Fig. 2*e* and *f*), the ferrite grains become more extended in the direction of the deformation and are broken into fragments. The proportion of HAB grows to 57%. The mean size of the grain-subgrain structure and of the grains decreases to 370 and 600 nm respectively. Further growth in the strain to $\varepsilon \sim 2.9$ increases the mean size of the grain-subgrain structure to 460 nm, while the mean grain size remains virtually unchanged (580 nm) (Fig. 2*g* and *h*). New virtually equiaxed grains form within the extended initial ferrite grains, which raises the fraction of HAB to 75% (Fig. 3*a*). Such changes in the microstructure indicate active occurrence of dynamic recrystallization during swaging to $\varepsilon \sim 2.9$.

When the deformation temperature is lowered to 500°C at $\varepsilon \sim 2.2$ (Fig. 2*c* and *d*), the mean size of the ferrite grains

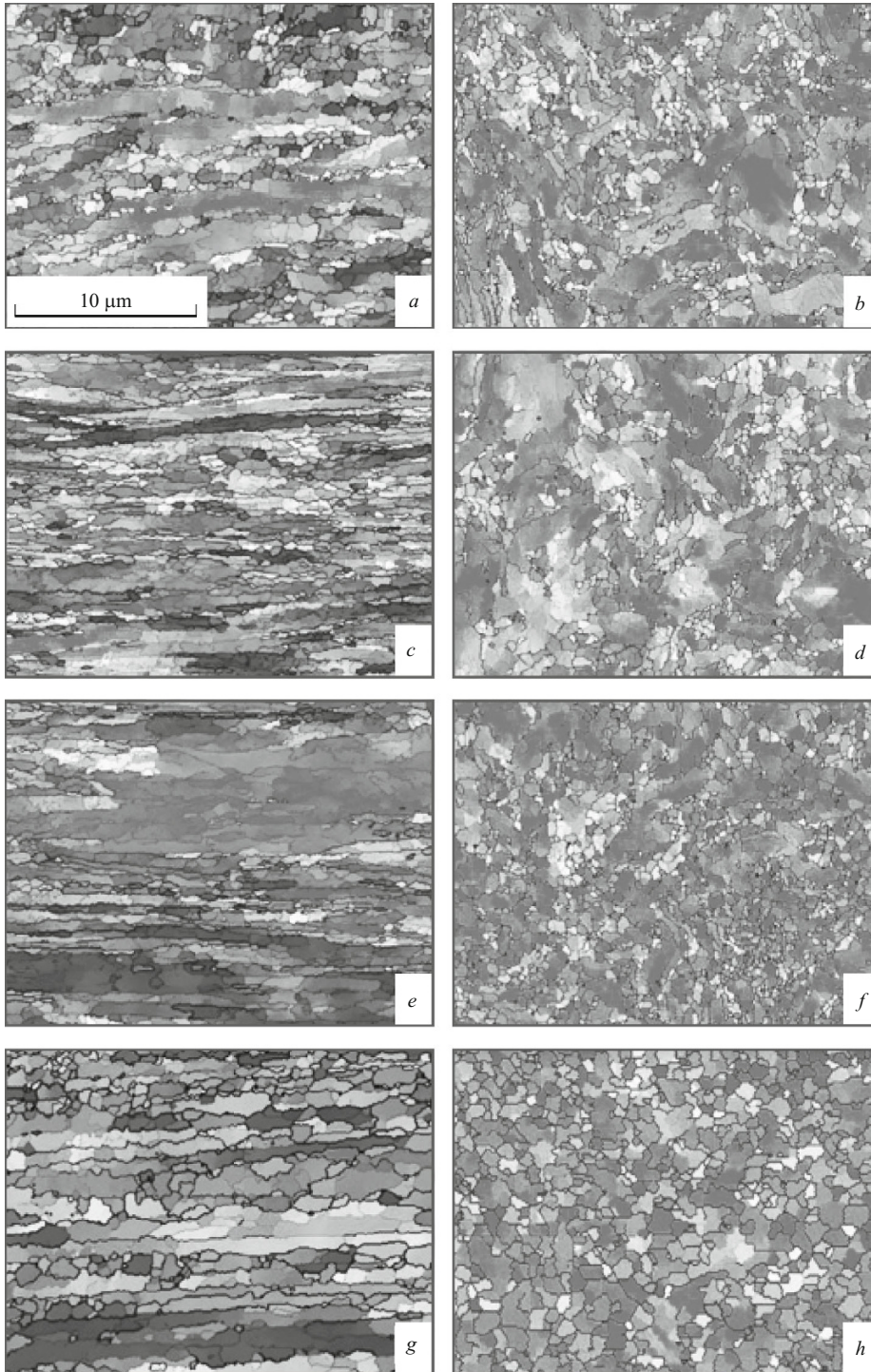


Fig. 2. Maps of orientation of grains/subgrains in longitudinal (*a, b, e, g*) and transverse (*c, d, f, h*) sections of steel 40KhGNM after swaging by different variants: *a, b*) $T = 600^{\circ}\text{C}$, $\varepsilon \sim 1.2$; *c, d*) $T = 500^{\circ}\text{C}$, $\varepsilon \sim 2.2$; *e, f*) $T = 600^{\circ}\text{C}$, $\varepsilon \sim 2.2$; *g, h*) $T = 500^{\circ}\text{C}$, $\varepsilon \sim 2.9$; *g, h*) $T = 600^{\circ}\text{C}$, $\varepsilon \sim 2.9$.

is 705 nm and does not change much as compared to that obtained after the deformation at 600°C . The mean size of the grain-subgrain structure decreases somewhat (from 420 nm at 600°C to 380 nm at 500°C), which agrees with the decrease in the fraction of HAB and the corresponding increase in the fraction of LAB (Fig. 3*a*). When the strain grows to the maximum value of $\varepsilon \sim 2.9$, the mean grain size decreases substantially (to 500 nm) at a virtually invariable mean size

of the grain-subgrain structure (400 nm). This may be a result of the development of recrystallization, which also follows from the growth of the fraction of HAB (Fig. 3*a*).

It should be noted that the mean size of ferrite grains at both deformation temperatures decreases depending on the degree of the deformation, and this effect is more pronounced when the deformation temperature is lowered from 600 to 500°C . This is connected with the difference in the ki-

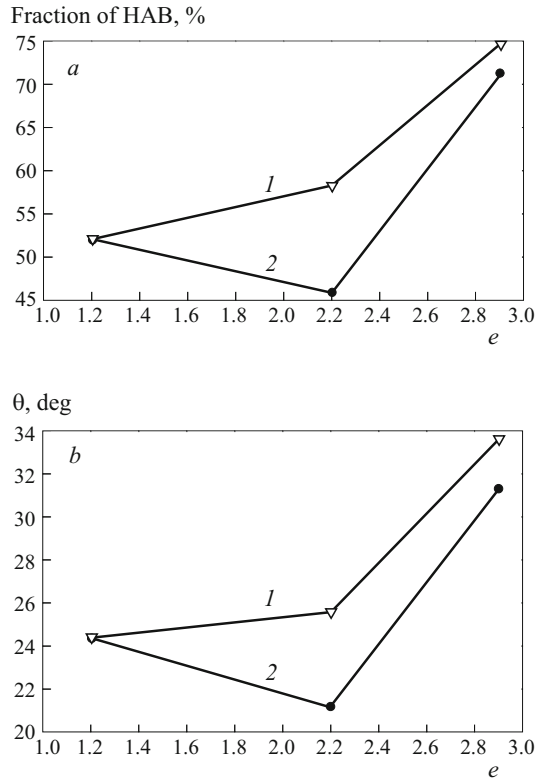


Fig. 3. Dependence of the proportion of HAB (*a*) and of the mean angle of off-orientation of grains/subgrains (*b*) on the true strain after swaging at 600°C (*1*) and at 600 → 500°C (*2*) (θ is the mean angle of off-orientation; ϵ is the true strain).

netics of structural rearrangement at different temperatures, which can be inferred from the dependence of the fraction of HAB and of the mean angle of off-orientation on the degree of deformation at both temperatures (Fig. 3*a* and *b*). The slower kinetics of formation of the UFG microstructure at 500°C than at 600°C is chiefly connected with the lower diffusion rates and shorter distances between the carbide particles. The measurements of the carbide particles after different variants of treatment prove the fact. For example, the mean size of carbides after the initial stage of the deformation at 600°C with $\epsilon \sim 1.2$ is about 45 nm. After the deformation at 500°C with $\epsilon \sim 2.2$ it is about 50 nm and remains virtually unchanged at $\epsilon \sim 2.9$ (about 55 nm). As a result of swaging at 600°C with $\epsilon \sim 2.2$ the mean size of the carbides is about 55 nm; after the deformation with $\epsilon \sim 2.9$ it grows to about 75 nm. Thus, the swaging temperature influences the microstructure substantially; though in both cases it causes formation of extended ferrite grains, the proportion of high-angle boundaries differs noticeably. Growth in the deformation temperature activates substantially the development of recrystallization and formation of new equiaxed grains.

Figure 4 presents the EBSD maps where grains with different orientations at deviation angle exceeding 10° are colored differently. The grains with direction indexed $\langle 110 \rangle$ are

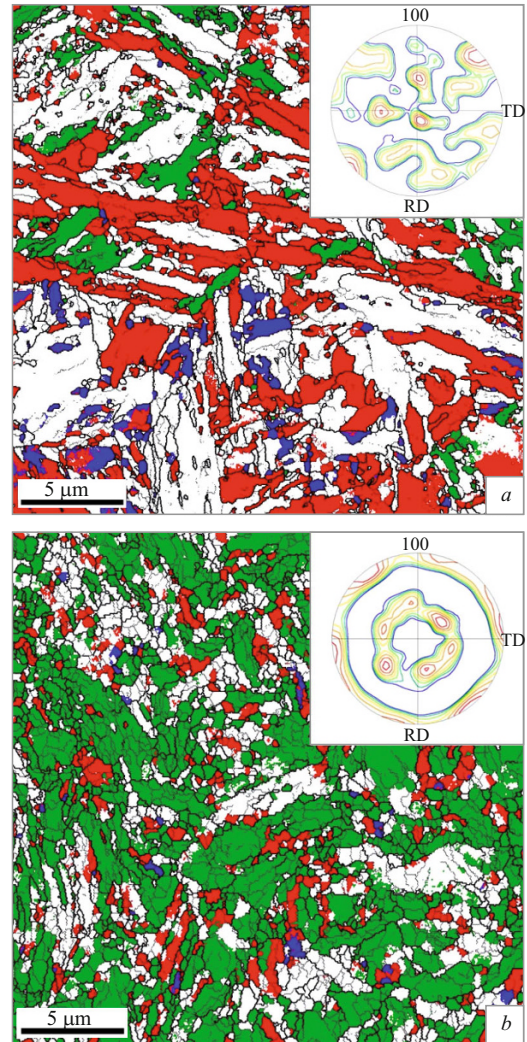


Fig. 4. Maps of distribution of texture components in steel 40KhGNM and pole figures before the start of deformation (*a*) and after swaging at 600°C with $\epsilon \sim 1.2$ (*b*). The grains with orientation $\langle 110 \rangle$ are colored green, the ones with orientation $\langle 123 \rangle$ are colored red, and the ones with orientation $\langle 112 \rangle$ are colored blue; the deviation angle is 10°.

colored green; those with index $\langle 123 \rangle$ are colored red, and those with index $\langle 112 \rangle$ are colored blue. It can be seen from Fig. 4*a* that before the deformation is started the structure is characterized by the following fractions of texture components: 4% $\langle 110 \rangle$, 19% $\langle 112 \rangle$, and 33% $\langle 123 \rangle$. During the swaging component $\langle 100 \rangle$ becomes dominant for all the regimes; the presence of $\langle 123 \rangle$ does not exceed 20%, and that of $\langle 112 \rangle$ is 3% (Fig. 4*b*).

Figure 5 presents the dependence of the fractions of texture components on the degree of deformation at different temperatures. It can be seen (Fig. 5*b*) that after the swaging without changing the temperature between the stages the fraction of component $\langle 110 \rangle$ increases monotonically from 58% after the first stage ($\epsilon \sim 1.2$) to 71% after the final stage

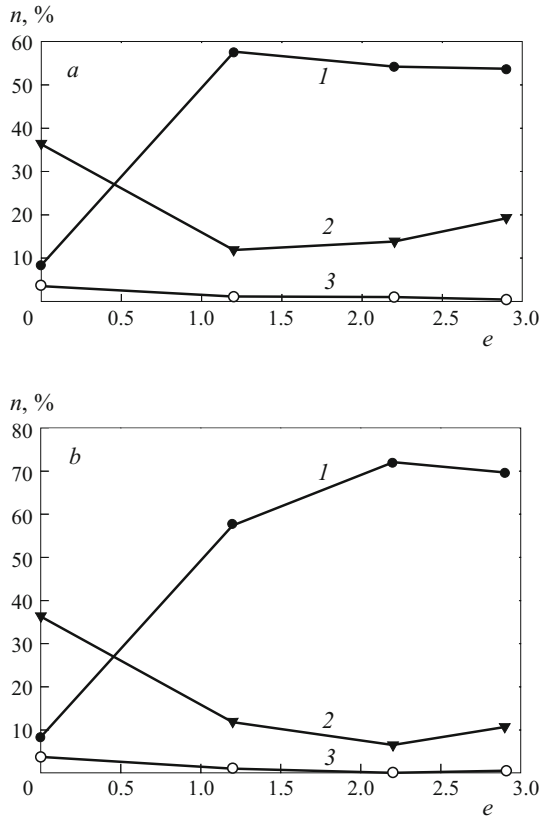


Fig. 5. Dependence of the fractions of texture components (n) on true strain (e): *a*) swaging at $600 \rightarrow 500^\circ\text{C}$; *b*) swaging at 600°C ; 1) $\langle 110 \rangle$; 2) $\langle 123 \rangle$, 3) $\langle 112 \rangle$.

($\varepsilon \sim 2.9$) The fractions of the other texture components remain virtually unchanged. After the swaging with decrease of the temperature (Fig. 5*a*) the fraction of component $\langle 110 \rangle$ does not change from the first stage to the last one and is equal to 55%. The fraction of component $\langle 112 \rangle$ remains virtually unchanged too, while the proportion of component $\langle 123 \rangle$ increases by 7%. Such distribution of texture components seems to be connected with the difference in the dominant mechanisms of structure formation developed at 500 and 600°C .

It can be seen from the pole figures that the specimens after swaging possess a strong axial texture. We should note that crack propagation over cleavage planes $\{100\}$ in steels

with bcc lattice requires much lower energy than crack propagation in plane $\{110\}$ of ductile fracture [8, 9]. With allowance for the presence of crystallographic and metallographic textures we may conclude that the formation of such microstructure should play some role in the development of fracture.

The results of the mechanical tests of specimens after different variants of swaging and after quenching and high tempering are presented in Table 1. The formation of UFG structure in the swaged specimens already after the deformation to $\varepsilon \sim 1.2$ ($T = 600^\circ\text{C}$) provides noticeable growth in the strength and ductility parameters as compared to the specimen after the conventional heat treatment (quenching and tempering). When the strain grows to $\varepsilon \sim 2.2$ at the same treatment temperature, the value of $\sigma_{0.2}$ increases additionally by 50 MPa and that of σ_r increases by 40 MPa; decrease in the treatment temperature from 600 to 500°C increases the strength characteristics by 110 and 80 MPa, respectively. The elongation does not change considerably in both cases. When the strain increases to $\varepsilon \sim 2.9$, the ductility grows by 2–5% at both temperatures, while the strength decreases noticeably, especially at 600°C , attaining values below those detected after the initial deformation stage. It seems that this effect is connected with enhancement of structural perfection and growth in the fraction of HAB.

The impact energy of the specimens after swaging increases by a factor of 3–4 at room temperature and by a factor of 15 at low temperatures (Table 2) as compared to the heat treated specimens. When the degree of the deformation is increased, the impact toughness grows substantially. The highest impact toughness is detected after swaging at $600^\circ\text{C} \rightarrow 500^\circ\text{C}$ with maximum strain. The impact toughness in the swaged condition does not decrease in the range of the brittle-to-ductile transition of the heat treated steel. The fracture surfaces of the specimens have a layered pattern, when the crack branches perpendicularly to the direction of the impact. This is a consequence of the orientation of cleavage planes $\{100\}$ in parallel to the longitudinal direction of the bar and of the extended shape of the ferrite grains, because the crack propagates chiefly over grain boundaries and hence over the length of the specimen. A similar type of fracture has been detected in [6, 10, 11] after tempforming,

TABLE 1. Mechanical Properties of Steel 40KhGNM after Different Swaging Stages

Swaging regime	$\sigma_{0.2}$, MPa	σ_r , MPa	δ , %	KV , J
Quenching from 840°C + 1-h tempering at 600°C	820	980	15	58
$T = 600^\circ\text{C}$, $\varepsilon \sim 1.2$	980	1020	18	143
$T = 600^\circ\text{C}$, $\varepsilon \sim 1.2 \rightarrow T = 500^\circ\text{C}$, $\varepsilon \sim 2.2$	1090	1100	17	158
$T = 600^\circ\text{C}$, $\varepsilon \sim 2.2$	1030	1060	16	212
$T = 600^\circ\text{C}$, $\varepsilon \sim 1.2 \rightarrow T = 500^\circ\text{C}$, $\varepsilon \sim 2.9$	960	1000	19	235
$T = 600^\circ\text{C}$, $\varepsilon \sim 2.9$	830	900	22	223

TABLE 2. Effect of Regimes of Swaging on the Impact Energy in the Range of Low Temperatures

Swaging regime	Impact energy, J, at a temperature of, °C				
	+20	-20	-40	-65	-100
Quenching from 840°C + 1-h tempering at 600°C	58	37	30	26	18
$T = 600^{\circ}\text{C}$, $\varepsilon \sim 1.2 \rightarrow T = 500^{\circ}\text{C}$, $\varepsilon \sim 2.2$	158	146	169	206	122
$T = 600^{\circ}\text{C}$, $\varepsilon \sim 2.2$	212	219	198	267	183
$T = 600^{\circ}\text{C}$, $\varepsilon \sim 1.2 \rightarrow T = 500^{\circ}\text{C}$, $\varepsilon \sim 2.9$	235	278	202	280	291
$T = 600^{\circ}\text{C}$, $\varepsilon \sim 2.9$	223	258	270	217	261

where the impact energy grew by a factor of 16 as compared to the state after quenching and tempering.

CONCLUSIONS

1. Swaging of preliminarily quenched steel 40KhGNM in the range of 600–500°C produces an extended UFG structure with carbides dispersed in ferrite grains. After the swaging at constant temperature $T = 600^{\circ}\text{C}$ to strain $\varepsilon \sim 2.9$ the mean size of the ferrite grains in cross section is 580 nm and that of the carbides is 75 nm. After the swaging by regime 600°C → 500°C the mean size of the ferrite grains is 500 nm and that of the carbides is 55 nm. The difference in the size of the ferrite grains is connected with the occurrence of recrystallization at 600°C.

2. The combination of microstructural factors after swaging, i.e., a well manifested axial texture, extended ferrite grains and relatively uniform distribution of nanosize carbides, provides elevation of the strength and impact toughness as compared to the state of the steel after quenching and high tempering. The best combination of the characteristics of strength, ductility and impact toughness of the metal at room temperature is obtained after swaging in the mode of 600°C → 500°C, namely, $\sigma_{0.2} = 960$ MPa, $\sigma_r = 1000$ MPa, $\delta = 19\%$, and $KV = 235$ J, whereas after the toughening $\sigma_{0.2} = 820$ MPa, $\sigma_r = 980$ MPa, $\delta = 15\%$ and $KV = 58$ J. The impact toughness in the range of the brittle-to-ductile transition in the swaged steel does not decrease with decrease in the test temperature, like in the toughened steel, but rather grows exceeding the value in the toughened condition at -100°C by a factor of 14–16.

The work has been performed with financial support of the Ministry of Education and Science of the Russian Federation (Contract No. 11.1816.2014/K). The authors are grate-

ful to the Center of Collective Use of Scientific Equipment of the Belgorod State National Research University "Diagnostics of the Structure and Properties of Nanomaterials" for the help with the instrumental analysis.

REFERENCES

- O. V. Kudryashova, M. A. Gervas'ev, and Yu. V. Khudorozhkova, "Structure and properties of medium-carbon Cr – Ni – Mo steel with Al and Si additives after quenching from the double-phase range," *Fundament. Issled.*, No. 4, 580 – 585 (2013).
- B. I. Arzamasov, V. I. Makarova, G. G. Mukhin, et al., *The Science of Materials* [in Russian], MGTU Im. N. E. Bauman, Moscow (2008), 648 p.
- Superfine Grains in Metals* [in Russian], Metallurgiya, Moscow (1973), 384 p.
- R. W. Hertzberg, *Deformation and Fracture Mechanics of Engineering Materials* (1996), 786 p.
- R. Song, D. Ponge, D. Raabe, et al., "Overview of processing, microstructure and mechanical properties of ultrafine grained bcc steels," *Mater. Sci. Eng. A*, **441**, 1 – 17 (2006).
- Y. Kimura, T. Inoue, F. Yin, and K. Tsuzaki, "Inverse temperature dependence of toughness in an ultrafine grain," *Science*, **320**, 1057 – 109 (2008).
- C. Week, *Treatment of Metals without Chipping* [Russian translation], Mir, Moscow (1965), 549 p.
- G. I. Bel'chenko and S. I. Gubenko, *Fundamentals of Metallography and Plastic Deformation of Steel* [in Russian], Vishcha Shkola, Kiev – Donetsk (1987), 240 p.
- H. Bhadeshia and R. Honeycombe, *Steels: Microstructure and Properties* (2006), 306 p.
- Y. Kimura, T. Inoue, F. Yin, and K. Tsuzaki, "Delamination toughening of ultrafine grain structure steels processed through tempforming at elevated temperatures," *ISIJ Int.*, **50**, 152 – 161 (2010).
- Y. Kimura and T. Inoue, "Influence of warm tempforming on microstructure and mechanical properties in an ultrahigh-strength medium-carbon low-alloy steel," *Metall. Mater. Trans. A*, **44**, 560 – 576 (2013).